A Novel Targeting Therapy of Malignant Mesothelioma Using Anti-Podoplanin Antibody

Shinji Abe,* Yuki Morita,† Mika Kato Kaneko,‡ Masaki Hanibuchi,§ Yuta Tsujimoto,‡ Hisatsugu Goto,§ Soji Kakiuchi,§,¶ Yoshinori Aono,§ Jun Huang,§ Seidai Sato,§ Masatoshi Kishuku,† Yuki Taniguchi,† Mami Azuma,* Kazuyoshi Kawazoe,† Yoshitaka Sekido,‖ Seiji Yano,# Shin-ichi Akiyama,¶ Saburo Sone,§,¶ Kazuo Minakuchi,† Yukinari Kato,‡ and Yasuhiko Nishioka§

Podoplanin (Aggrus), which is a type I transmembrane sialomucin-like glycoprotein, is highly expressed in malignant pleural mesothelioma (MPM). We previously reported the generation of a rat anti-human podoplanin Ab, NZ-1, which inhibited podoplanin-induced platelet aggregation and hematogenous metastasis. In this study, we examined the antitumor effector functions of NZ-1 and NZ-8, a novel rat-human chimeric Ab generated from NZ-1 including Ab-dependent cellular cytotoxicity (ADCC) and complement-dependent cytotoxicity against MPM in vitro and in vivo. Immunostaining with NZ-1 showed the expression of podoplanin in 73% (11 out of 15) of MPM cell lines and 92% (33 out of 36) of malignant mesothelioma tissues. NZ-1 could induce potent ADCC against podoplanin-positive MPM cells mediated by rat NK ($CD161a^+$) cells, but not murine splenocytes or human mononuclear cells. Treatment with NZ-1 significantly reduced the growth of s.c. established tumors of MPM cells (ACC-MESO-4 or podoplanin-transfected MSTO-211H) in SCID mice, only when NZ-1 was administered with rat NK cells. In in vivo imaging, NZ-1 efficiently accumulated to xenograft of MPM, and its accumulation continued for 3 wk after systemic administration. Furthermore, NZ-8 preferentially recognized podoplanin expressing in MPM, but not in normal tissues. NZ-8 could induce higher ADCC mediated by human NK cells and complement-dependent cytotoxicity as compared with NZ-1. Treatment with NZ-8 and human NK cells significantly inhibited the growth of MPM cells in vivo. These results strongly suggest that targeting therapy to podoplanin with therapeutic Abs (i.e., NZ-8) derived from NZ-1 might be useful as a novel immunotherapy against MPM. ***The Journal of Immunology*****, 2013, 190: 6239–6249.**

Malignant pleural mesothelioma (MPM) is an aggressive malignancy arising from the mesothelial cells lining the pleura (1). Previously, MPM was considered to be rare; however, its incidence is increasing worldwide. According to various studies, the number of cases is estimated to reach a peak between 2010 and 2020 in Europe (2) and ~2030–2040 in Asia (3). Despite the combined therapies including surgery, radiotherapy, and chemotherapy, the prognosis of MPM is very poor: median survival from the time of diagnosis is 4–12 mo, and the 5-y survival rate is <5% (4–6). Therefore, novel therapeutic strategies for MPM are urgently necessary for improving the prognosis.

On the basis of the current status of MPM, immunotherapy has also been considered as one of the novel therapeutic approaches. Recently, tumor-specific immunotherapy using vaccination with antigenic peptides of tumor-associated Ags (TAAs) with or without dendritic cells or Abs has been conducted because several TAAs specific for MPM were reported, although their number is insufficient (7–9). Among them, immunotherapy with specific Abs seems to be the most promising approach, whereas clinical trials with humanized Abs for mesothelin as well as CD26 are still in phase I (10).

Podoplanin (Aggrus), which is a type I transmembrane sialomucin-like glycoprotein, induces platelet aggregation (11–14). Originally, podoplanin was detected on the surface of podocytes (15). Although podoplanin is reported to be expressed in limited normal tissues such as endothelium of lymphatic vessels and in type I alveolar epithelium (16, 17), various tumors such as squamous cell carcinomas, testicular seminomas, malignant brain tumors, fibrosarcomas, and malignant mesotheliomas (MMs) including MPM are known to show its overexpression (18–22). Furthermore, it has been reported that podoplanin is associated with cell migration (23, 24), epithelial–mesenchymal transition (25), and tumor metastasis (26, 27). Moreover, podoplanin serves through extra-

*Central Office for Clinical Pharmacy Training, Institute of Health Biosciences, University of Tokushima Graduate School, Tokushima 770-8503, Japan; †Department of Pharmacy, Tokushima University Hospital, Tokushima 770-8503, Japan; ‡Regional Innovation Strategy Support Program, Tohoku University Graduate School of Medicine, Sendai 980-8575, Japan; §Department of Respiratory Medicine and Rheumatology, Institute of Health Biosciences, University of Tokushima Graduate School, Tokushima 770-8503, Japan; ¶Department of Medical Oncology, Institute of Health Biosciences, University of Tokushima Graduate School, Tokushima 770-8503, Japan; ‖Division of Molecular Oncology, Aichi Cancer Center Research Institute, Nagoya 464-8681, Japan; and #Division of Medical Oncology, Cancer Research Institute, Kanazawa University, Kanazawa 920-1192, Japan

Received for publication February 15, 2013. Accepted for publication March 17, 2013.

This work was supported in part by Kakenhi (Grants 24390210, 22390166, 23790185, 23701043, and 23791584), a Grant-in-Aid for Scientific Research (B) (to Y.N. and S.S.) and Grants-in-Aid for Young Scientists (B) (to S.A., M.K.K., and Y.K.) from the Ministry of Education, Culture, Sports, Science and Technology of Japan, the Mitsubishi Pharma Research Foundation (to Y.K.), the Children's Cancer Association of Japan (to Y.K.), the Intelligent Cosmos Academic Foundation (to Y.K.), the Platform for Drug Discovery, Informatics, and Structural Life Science (to M.K.K. and Y.K.), and the Regional Innovation Strategy Support Program (to Y.K.).

Address correspondence and reprint requests to Prof. Yasuhiko Nishioka, Department of Respiratory Medicine and Rheumatology, Institute of Health Biosciences, University of Tokushima Graduate School, 3-18-15 Kuramoto-cho, Tokushima 770-8503, Japan. E-mail address: yasuhiko@clin.med.tokushima-u.ac.jp

Abbreviations used in this article: ADCC, Ab-dependent cellular cytotoxicity; CDC, complement-dependent cytotoxicity; CHO, Chinese hamster ovary; CRPMI 1640, RPMI 1640 medium supplemented with 10% FBS; MM, malignant mesothelioma; MNC, mononuclear cell; MPM, malignant pleural mesothelioma; MSFI, mean specific fluorescence intensity; PDPN, podoplanin; TAA, tumor-associated Ag.

cellular matrix signaling pathways for cell cycle and cell proliferation (28), and increase of expression of podoplanin is also related to tumor malignancy and poor clinical outcome (22, 29, 30).

To establish targeted therapy to podoplanin, we previously generated a rat anti-human podoplanin mAb NZ-1 (31, 32). NZ-1 suppressed podoplanin-induced pulmonary metastasis by inhibiting tumor-induced platelet aggregation (27). Furthermore, we showed that NZ-1 has not only high specificity and sensitivity but also high binding affinity against podoplanin, leading to its status as a candidate for radioimmunotherapy or immunotoxin therapy (33). However, it has not been clarified whether NZ-1 has antitumor effector functions including Ab-dependent cellular cytotoxicity (ADCC) and complement-dependent cytotoxicity (CDC), which is the most important mechanism contributing to the clinical efficacy of therapeutic Abs (34).

In the current study, we investigated whether NZ-1 can induce antitumor effects mediated by ADCC and CDC against MPM in vitro and in vivo. Furthermore, we also evaluated antitumor activity of NZ-8, a novel rat-human chimeric anti-human podoplanin Ab, using human mononuclear cells (MNC) as effector cells against MPM cells.

Materials and Methods

Cell lines

In this study, we used 15 human MPM cell lines. ACC-MESO-1, ACC-MESO-4, Y-MESO-8A, Y-MESO-9, Y-MESO-12, and Y-MESO-14 were established in Aichi Cancer Research Center Institute (35). EHMES-1 was provided by Dr. Hironobu Hamada (Ehime University, Matsuyama, Japan) (36). NCI-H290 and NCI-H513 were provided by Dr. Adi F. Gazdar (University of Texas Southwestern Medical Center, Dallas, TX). MSTO-211H, NCI-H28, NCI-H226, NCI-H2052, NCI-H2373, NCI-H2452, and Chinese hamster ovary (CHO) were purchased from American Type Culture Collection (Rockville, MD). MPM cell lines are divided into three histological origins, an epithelioid type (ACC-MESO-1, ACC-MESO-4, Y-MESO-9, Y-MESO-12, NCI-H290, NCI-H513, NCI-H226, and NCI-H2452), a sarcomatoid type (NCI-H28, NCI-H2052, and NCI-H2373), and a biphasic type (Y-MESO-8A, Y-MESO-14, EHMES-1, and MSTO-211H) (37–39). These cells were cultured in RPMI 1640 medium supplemented with 10% FBS (CRPMI 1640; Life Technologies, Grand Island, NY), 100 U/ml penicillin, and 100 μg/ml streptomycin (Meiji Seika Kaisha, Tokyo, Japan). Cell lines were authenticated by DNA fingerprinting. MSTO-211H cells were transfected with appropriate amounts of plasmids, pcDNA3/human podoplanin (PDPN) or pcDNA3/mock (11), using Metafectene (Nippon Genetics, Tokyo, Japan) according to the manufacturer's instructions. Stable transfectants (MSTO-211H/PDPN and MSTO-211H/mock) were selected by cultivating the transfectants in medium containing 0.5 mg/ml Geneticin (Invitrogen, Carlsbad, CA).

Abs

NZ-1, a rat anti-human podoplanin mAb (IgG_{2a}), was developed as described previously (31). Rat IgG and human IgG were purchased from Beckman Coulter (Fullerton, CA). For the generation of rat-human chimera anti-human podoplanin (NZ-8), the appropriate V_H and V_L cDNAs of a rat NZ-1 Ab and C_H and C_L of human IgG_1 were subcloned into the pcDNA3.3/Neo or pcDNA3.1/Zeo vectors (Life Technologies), respectively. The cDNAs coding for the V_H and V_L (κ-chain) regions were constructed by a PCR-based method. Ab expression vectors were transfected into CHO cells using Lipofectamine 2000 reagent (Life Technologies). Stable transfectants of CHO/NZ-8 were selected by cultivating the transfectants in medium containing 1 mg/ml Geneticin and 0.5 mg/ml Zeocin (Life Technologies). CHO/NZ-8 cells were cultivated in CHO-S-SFM II medium (Life Technologies). The media containing NZ-8 were centrifuged, and the obtained supernatant was applied to a column of protein G-Sepharose (Thermo Scientific, Rockford, IL). After extensive washing with PBS, the fusion proteins were eluted using 0.1 M glycine and 0.15 M NaCl (pH 2.8) and then neutralized with 1 M Tris (pH 10). The Abs were dialyzed against PBS. Expression and purity of the proteins were confirmed by SDS-PAGE using 5–20% gradient gels (Wako Pure Chemical Industries, Osaka, Japan). $F(ab')_2$ fragments of NZ-1 Ab were prepared using $F(ab')_2$ Preparation Kits (Thermo Scientific) according to the manufacturer's instructions. D2-40 (mouse anti-human podoplanin mAb) was purchased from DakoCytomation (Glostrup, Denmark).

Animals

Male SCID mice, 5 to 6 wk old, and male Wistar rats, 6 wk old, were obtained from CLEA Japan (Osaka, Japan) and maintained under specific pathogen-free conditions throughout this study. All animals were acclimatized for at least 1 wk before experiments. All experiments were performed in accordance with the guidelines of University of Tokushima, Committee on Animal Care and Use.

Flow cytometry

Expression of podoplanin was detected by flow cytometry. Cells (5×10^5) were washed with cold PBS and stained on ice for 30 min with NZ-1 (1 μg/ml), NZ-1 $F(ab')_2$ fragment (0.675 μg/ml), NZ-8 (1 μg/ml), rat IgG (1 μg/ml), or human IgG (1 μg/ml). After incubation with the primary mAbs, cells were washed with cold PBS and then incubated on ice for 30 min with FITC-conjugated goat $F(ab')_2$ fragment anti-rat IgG (H+L) Ab or FITC-conjugated goat $F(ab')_2$ Fragment anti-human IgG (Fcγ) Ab (Beckman Coulter). The cells were washed again and resuspended in cold PBS. The analysis was performed on an FACSCalibur flow cytometer with CellQuest software (BD Biosciences, Franklin Lakes, NJ). The mean specific fluorescence intensity (MSFI) was calculated as the ratio of the mean fluorescence intensity of NZ-1 to that of control mAb. Positive expression of podoplanin was defined as an MSFI of >2.0, and high-level expression of podoplanin was defined as an MSFI of >10.0.

Immunohistochemistry

Tissue arrays of human mesothelioma were obtained from Biomax (Rockville, MD). Staining was performed using R.T.U. VECTASTAIN Elite ABC Kit (Vector Laboratories, Burlingame, CA) (40). The tissue arrays were steamed in sodium citrate buffer for 10 min using a microwave to retrieve Ag and incubated in 3% H_2O_2 for 30 min to inhibit endogenous peroxidase. After incubation in blocking serum for 20 min, the slides were incubated overnight with NZ-1, NZ-8, or D2-40 at 4°C. The slides were washed and incubated in prediluted biotinylated secondary Ab for 30 min, followed by incubation in ready-to-use streptavidin/peroxidase complex reagent for 30 min. The tissue arrays were developed with a diaminobenzidine substrate kit (Vector Laboratories) and counterstained with Mayer's hematoxylin (Muto Pure Chemicals, Tokyo, Japan).

Western blotting

Cells were rinsed with ice-cold PBS and lysed in M-PER reagent (Pierce, Rockford, IL) containing phosphatase and protease inhibitor cocktails (Roche, Indianapolis, IN). The concentrations of protein were determined using a Bio-Rad Protein Assay Kit (Bio-Rad, Hercules, CA). Cell lysate (15 μg/lane) was separated by SDS-PAGE. Immunoblotting was conducted as previously described (41).

Preparation of effector cells

Rat splenocytes were harvested from Wistar rat spleens. Spleens were minced, homogenized in RPMI 1640, and centrifuged after passing through the cell strainer (BD Biosciences) (40). The cell pellet was suspended in RBC lysis buffer (Sigma-Aldrich, St. Louis, MO) on ice for 10 min. After depletion of RBCs, splenocytes were resuspended in CRPMI 1640 and used as effector cells. The method by which SCID mouse splenocytes were harvested was the same as that of rat splenocytes. Human PBMCs (MNC) were obtained from leukocytes in lymphocyte separation medium (Litton Bionetics, Kensington, MD) as previously described (42). Leukocytes were separated from peripheral blood of healthy donors using an RS-6600 rotor of a Kubota KR-400 centrifuge (Kubota, Tokyo, Japan). The human study was approved by the ethics committee of University of Tokushima, and written informed consent was obtained from all of the subjects.

ADCC

ADCC was evaluated using a [^{51}Cr]release assay as described previously (40, 43). Target cells were targeted with 0.1 μCi [^{51}Cr]sodium chromate at 37°C for 1 h. ^{51}Cr-labeled target cells were placed in 96-well plates in triplicate. Effector cells and NZ-1, NZ-1 $F(ab')_2$ fragment, NZ-8, or control IgG were added to the plates. After 6 h incubation, 100 μl supernatant was measured in a γ counter (PerkinElmer, Waltham, MA). Percent of cytotoxicity was calculated from the following formula: percent specific lysis = $(E - S)/(M - S) \times 100$, where E is the release in the test sample, S is the spontaneous release, and M is the maximum release.

Complement-dependent cytotoxicity

CDC was determined by [^{51}Cr]release assay (40). Target cells were incubated with 0.1 μCi [^{51}Cr]sodium chromate at 37°C for 1 h. After in-

cubation, the cells were washed with CRPMI 1640 three times. ^{51}Cr-labeled cells were added into 96-well plates and incubated with baby rabbit complement (Cedarlane Laboratories, Ontario, Canada) at a dilution of 1:4 and NZ-1 (1 μg/ml), NZ-8 (1 μg/ml), or control IgG (1 μg/ml) for 6 h. [^{51}Cr]Release of the supernatant from each well (100 μl) was measured using a γ counter. Percent of cytotoxicity was calculated as above.

Depletion or separation of rat NK cells

Depletion of NK cells from rat splenocytes was performed using the anti-asialo GM1 Ab as follows. Harvested rat splenocytes were treated with anti-asialo GM1 Ab (Wako, Osaka, Japan) at room temperature for 30 min. After treatment, splenocytes were incubated with baby rabbit complement at 37°C for 30 min, then washed with CRPMI 1640 three times, and the number of cells for use in experiments was counted. Rat NK cells were separated from Wistar rat splenocytes using a magnetic cell-sorting system. Splenocytes were incubated with FITC-conjugated anti-CD161a Ab (BD Biosciences) at 4°C for 30 min and then with anti-FITC mAb-coupled superparamagnetic microbeads (Miltenyi Biotec, Auburn, CA) at 4°C for 15 min. CD161a-positive or -negative selection was carried out using an autoMACS (Miltenyi Biotec) according to the manufacturer's instructions (44). Isolated CD161a$^+$ and CD161a$^-$ cells that yielded purity ≥90 and ≥99.9%, respectively, as determined by flow cytometry were used in experiments. To purify CD14$^+$ cells and CD56$^+$ cells from human MNC, AutoMACS and CD14 or CD56 microbeads (Miltenyi Biotec) were used. Human MNC were treated with CD14 or CD56 microbeads at 4°C for 15 min, and then cells were separated by autoMACS. The purities of CD14$^+$ and CD56$^+$ cells were ≥90%.

Animal experiments

SCID mice were injected s.c. into the right flank with ACC-MESO-4 (4.0×10^6 cells) or MSTO-211H/PDPN (1.0×10^6 cells). Tumor size is expressed as tumor area (mm^2): the longest diameter × the shortest diameter. The tumor-bearing mice were divided into several experimental groups before treatment with Abs was initiated. An i.p. injection of NZ-1 (100 μg), NZ-1

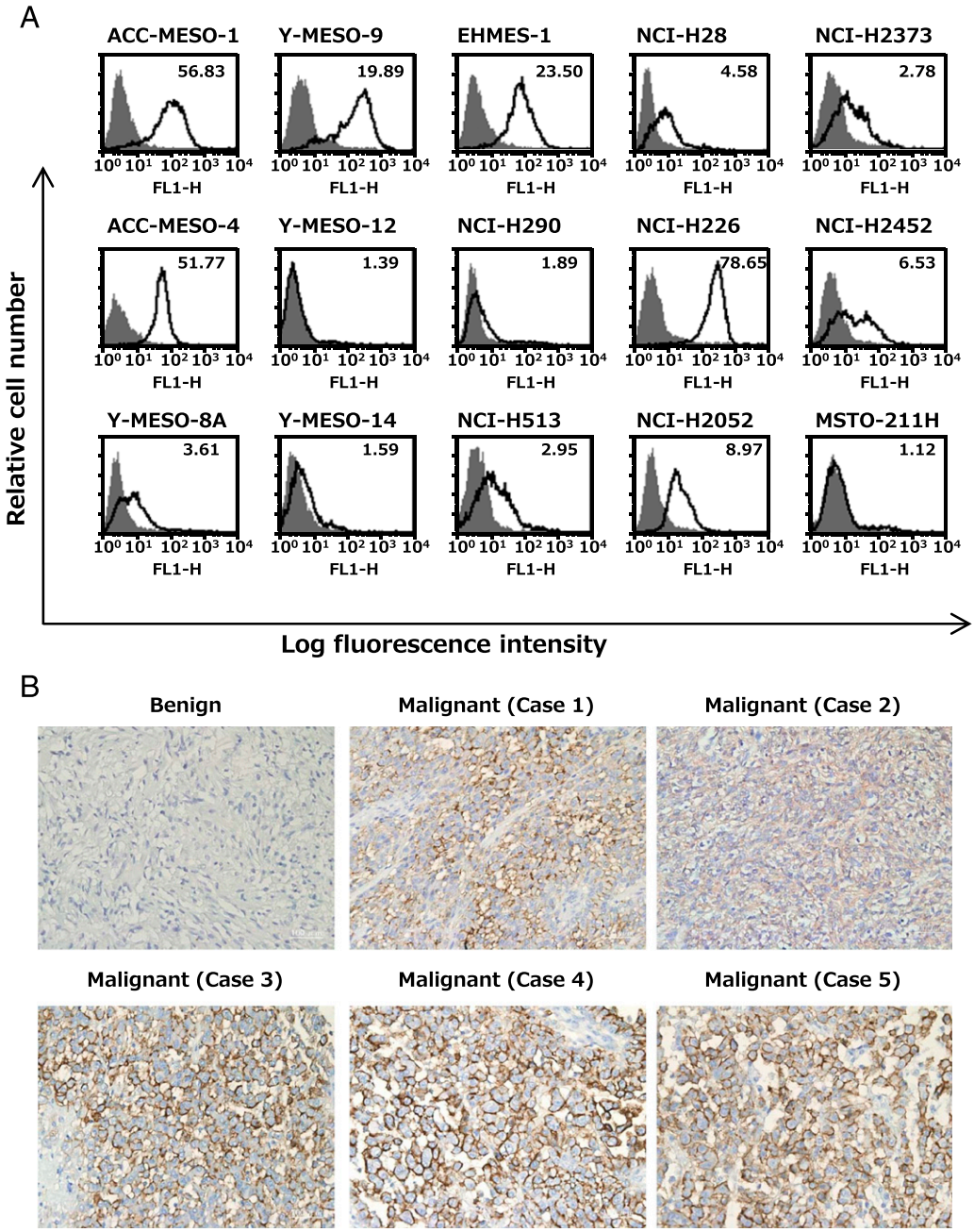

FIGURE 1. Expression of podoplanin in MM. (**A**) Expression of podoplanin in MPM cell lines was detected by flow cytometry. MPM cell lines were stained with NZ-1 (bold line) and control IgG (hatched area). The number in the top right corner in each figure is the MSFI. (**B**) Immunohistochemistry demonstrated the expression of podoplanin using the tissue array. Tissues were stained with 1 μg/ml of NZ-1 (original magnification ×200).

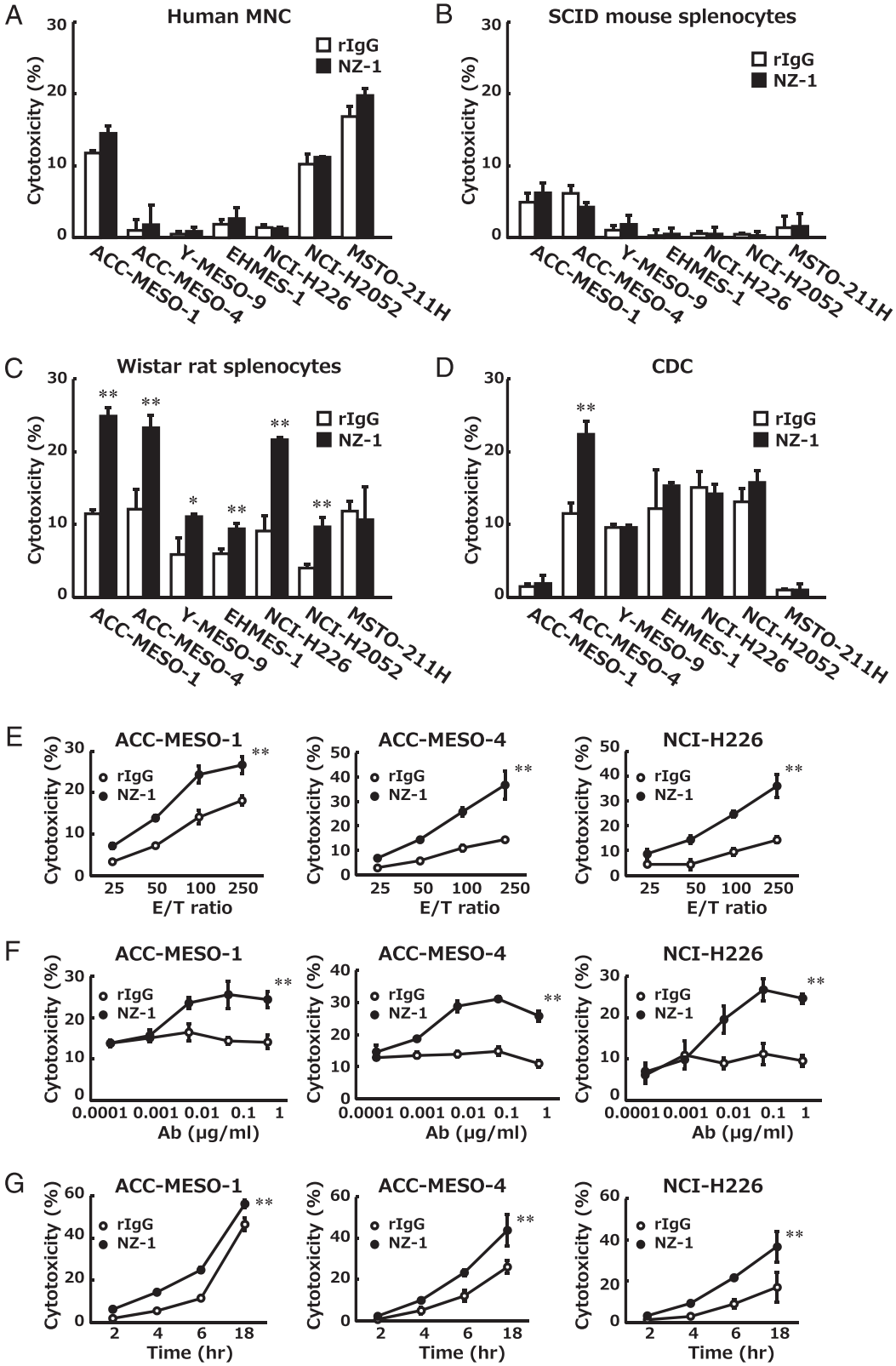

FIGURE 2. ADCC and CDC of NZ-1 against MPM cells. (**A**–**C**) ADCC activity of NZ-1 against various MPM cells was evaluated by 6-h [^{51}Cr]release assay in the presence of 1 μg/ml control rat IgG (rIgG; open column) or NZ-1 (filled column) at E:T ratio of 100. Human MNC (A), SCID mouse splenocytes (B), and Wistar rat splenocytes (C) were used as effector cells. (**D**) CDC activity of NZ-1 was determined using the 6-h [^{51}Cr]release assay in the presence of 1 μg/ml Ab with baby rabbit complement at a dilution of 1:4. E:T ratio (**E**) and dose dependence of NZ-1 (**F**) as well as time course of ADCC (**G**) were detected by [^{51}Cr]release assay using rat splenocytes as effector cells. Unchanged experimental conditions were 1 μg/ml Ab, 100 as the E:T ratio, and duration of 6 h. *$p < 0.05$ versus control, **$p < 0.01$ versus control (values are means ± SE).

$F(ab')_2$ fragment (67.5 μg), NZ-8 (100 μg), control rat IgG (100 μg), or control human IgG (100 μg) was started, on average, 14 d after tumor inoculation, when the tumor size had reached 15 (± 3 SD) mm^2, and continued twice a week for 2 wk. Rat $CD161a^+$ cells (1.0×10^5 cells), human $CD56^+$ cells (1.0×10^5 cells), or control normal saline injection (s.c.) around the tumors continued weekly for 2 wk.

In vivo fluorescence imaging

In vivo fluorescence imaging was performed using IVIS Spectrum (Caliper Life Sciences, Hopkinton, MA) (45). ACC-MESO-4 (4.0×10^6 cells) was injected into the right flank of SCID mice (s.c.). When the tumor grew to a sufficient size (25 mm^2), 100 μg NZ-1 or rat IgG labeled with XenoLight CF770 (Caliper Life Sciences) was injected (i.p.). The fluorescence in each mouse was determined using IVIS Spectrum (Caliper Life Sciences), with an excitation wavelength of 730–760 nm and an emission wavelength of 830–850 nm, every day after the labeled Ab injection. Mice were anesthetized with isoflurane (Abbott Laboratories, Chicago, IL). Images were acquired and analyzed using Living Image 3.1 software (Caliper Life Sciences).

Statistical analyses

The statistical significance of differences in in vitro and in vivo data were analyzed by Student *t* test and one-way ANOVA. In this study, *p* values <0.05 were considered significant in all experiments.

Results

Detection of podoplanin expression in MPM cell lines and tissues

First, we evaluated the expression of podoplanin on the surface of MPM cells using NZ-1, which is highly reactive for podoplanin. Fig. 1A shows that MPM cells expressed various levels of podoplanin as determined by flow cytometry. Expression of podoplanin was detected on 73% (11 out of 15) of MPM cells, and sarcomatoid type showed a higher expression rate of 100% (3 out of 3) as compared with 75% of epithelioid type (6 out of 8) and 50% of biphasic type (2 out of 4), although the number of cell lines is not sufficient to determine the expression rate. High level of expression of podoplanin, which is defined as a ratio of the mean fluorescence intensity of NZ-1 to that of control IgG of >10, was found in 33% (5 out of 15) of all cells, of which four cell lines are in an epithelioid type.

We next examined podoplanin expression in tissues of mesothelioma by immunohistochemistry with NZ-1. As shown in Fig. 1B, strong intensity of podoplanin staining was observed in tissues of MM, except benign mesothelioma. Podoplanin expression was found in 92% (33 out of 36) of all MM tissues.

ADCC and CDC mediated by NZ-1 against MPM cells

Next, we attempted to clarify whether NZ-1 has the potential to induce ADCC-targeted MPM cells expressing podoplanin. As shown in Fig. 2A and 2B, using human MNC or SCID mouse splenocytes as effector cells, we could not detect ADCC induced by NZ-1. By contrast, significant ADCC against only podoplanin-positive, but not podoplanin-negative, MPM cells was induced by NZ-1 when splenocytes of Wistar rat were used as effector cells (Fig. 2C). The level of ADCC was strongly associated with the level of podoplanin expression (Figs. 1A, 2C). In contrast, CDC induced by NZ-1 was detected only against ACC-MESO-4 cells (Fig. 2D). Additionally, treatment with 1 μg/ml NZ-1 alone did not inhibit proliferation of these MPM cell lines, indicating that NZ-1 has no direct growth-inhibitory activity on MPM cells in our experimental conditions (data not shown).

To evaluate the kinetics of ADCC activity mediated by NZ-1, we analyzed the E:T ratio and time course of ADCC and dose dependence of NZ-1. As shown in Fig. 2E, the level of ADCC was dependent on E:T ratio. In addition, NZ-1 also effectively induced ADCC against podoplanin-expressing cells in a dose- and time-dependent manner (Fig. 2F, 2G). The optimal concentration of NZ-1 to induce ADCC seems to be >0.1 μg/ml. These results suggest that rat anti-podoplanin Ab NZ-1 exhibits potent ADCC against MPM cells.

NZ-1 induces ADCC against podoplanin-transfected MPM cell lines

To confirm that ADCC of NZ-1 depends on the expression of podoplanin on target cells, we used MSTO-211H/PDPN as target

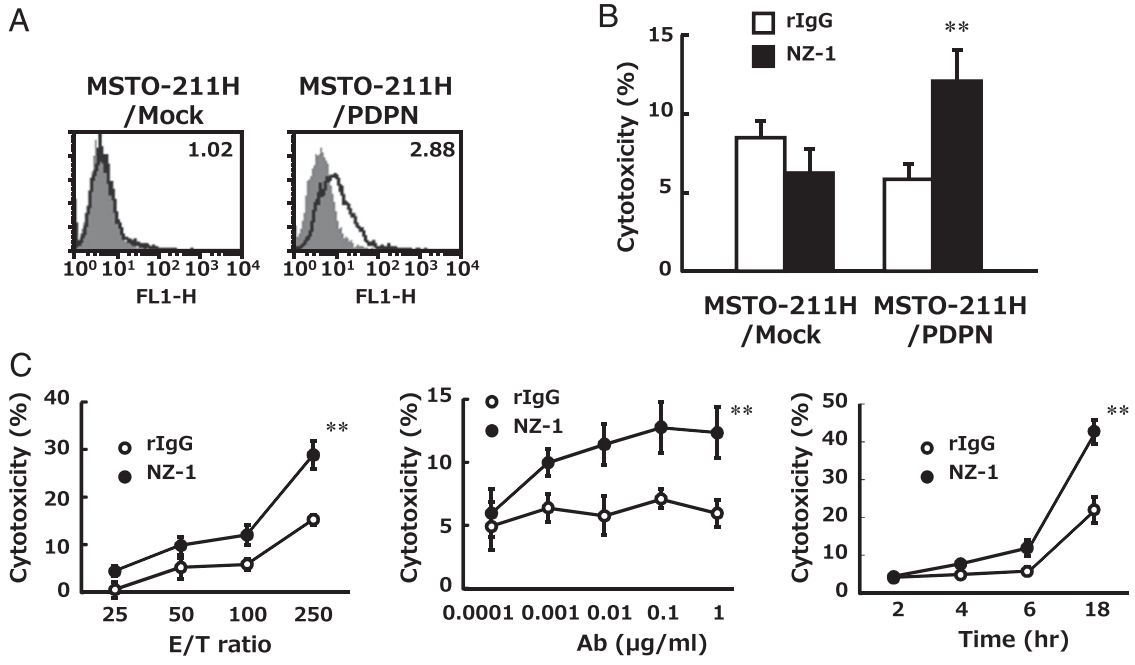

FIGURE 3. NZ-1 induces ADCC against MSTO-211H transfected with podoplanin. (**A**) Expression of podoplanin was detected by FACS analysis. (**B**) ADCC activity of NZ-1 using rat splenocytes against MSTO-211H/PDPN was evaluated by 6-h [^{51}Cr]release assay in the presence of 1 μg/ml Ab at the E:T ratio of 100. (**C**) E:T ratio–, dose-, and time-dependent effects of ADCC against MSTO-211H/PDPN mediated by NZ-1 with rat splenocytes were demonstrated by [^{51}Cr]release assay. $^{**}p < 0.01$ versus control (values are means ± SE). rIgG, rat IgG.

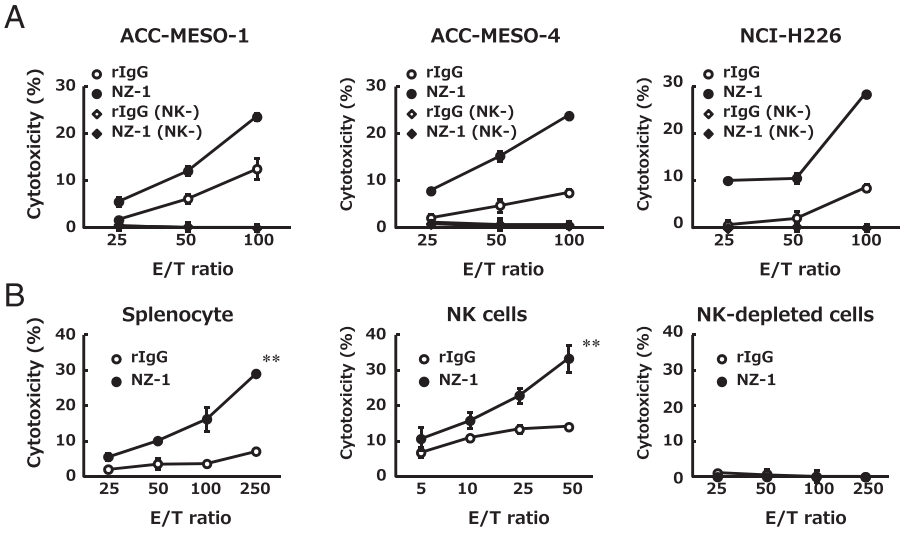

FIGURE 4. Rat NK cells are the main effector cells in ADCC induced by NZ-1. (**A**) Effects of depletion of NK cells from rat splenocytes on ADCC by NZ-1. NK cells in rat splenocytes were depleted by treatment of anti-asialo GM1 Ab and baby rabbit complement. (**B**) Rat NK cells are involved in ADCC activity of NZ-1. NK ($CD161a^+$) cells or NK-removed ($CD161a^-$) cells were isolated from rat splenocytes by AutoMACS. ADCC activity of 1 μg/ml Ab for 6 h was examined in ACC-MESO-4 as a target cell. $^{**}p < 0.01$ versus control (values are means ± SE). rIgG, Rat IgG.

cells. MSTO-211H/PDPN was generated by transfecting pcDNA3/podoplanin into MSTO-211H, one of the podoplanin-negative MPM cell lines (Fig. 3A). Although ADCC of NZ-1 was not detected against MSTO-211H/Mock, NZ-1 exhibited significant ADCC activity against MSTO-211H/PDPN (Fig. 3B). E:T ratio–, dose-, and time-dependent ADCC activities against MSTO-211H/PDPN were also induced by NZ-1 (Fig. 3C).

ADCC of NZ-1 is mediated by rat NK cells

For further investigation of the type of effector cells in rat splenocytes, we depleted NK cells using anti-asialo GM1 Ab and baby rabbit complement. As shown in Fig. 4A, ADCC was not induced by NK cell–depleted splenocytes. Moreover, we isolated NK ($CD161a^+$) cells and examined ADCC using NZ-1 against ACC-MESO-4. Fig. 4B shows that the purified NK ($CD161a^+$) cells from rat splenocytes showed a significant level of ADCC. In contrast, $CD161a^-$ splenocytes did not induce ADCC by NZ-1.

Antitumor activity of NZ-1 on the growth of podoplanin-expressing MPM cells in vivo

To evaluate the antitumor activity of NZ-1 in vivo, we used s.c. xenograft of human MPM (ACC-MESO-4) in SCID mice. NZ-1 or control rat IgG was injected i.p. twice a week, and rat NK ($CD161a^+$) cells or normal saline was injected s.c. weekly for 2 wk because ADCC of NZ-1 was mediated only by rat NK cells but not mouse splenocytes. Treatment with NZ-1 was started when tumors were established and formed a visible tumor mass (>15 mm^2) owing to the evaluation of therapeutic antitumor ability of NZ-1. The antitumor activity of NZ-1 against ACC-MESO-4 in vivo is shown in Fig. 5A. Administration of NZ-1 with rat NK ($CD161a^+$) cells significantly inhibited the growth of ACC-MESO-4 cells. By contrast, the injection of neither NZ-1 nor NK ($CD161a^+$) cells alone showed antitumor effects in our experimental setting. Using an MSTO-211H/PDPN xenograft model, tumor growth was also significantly inhibited by treatment with NZ-1 and NK ($CD161a^+$) cells (Fig. 5B).

Critical contribution of Fc portion to antitumor activity of NZ-1

It is known that ADCC activity is mediated by binding of the Fc portion of Abs to the FcR on NK cells. Therefore, we examined the antitumor activity of NZ-1 $F(ab')_2$ fragment. Although the NZ-1 F $(ab')_2$ fragment recognized podoplanin on ACC-MESO-4 in flow cytometric analysis to a similar extent as intact NZ-1, the $F(ab')_2$ fragment did not induce ADCC against ACC-MESO-4 (Fig. 6A,

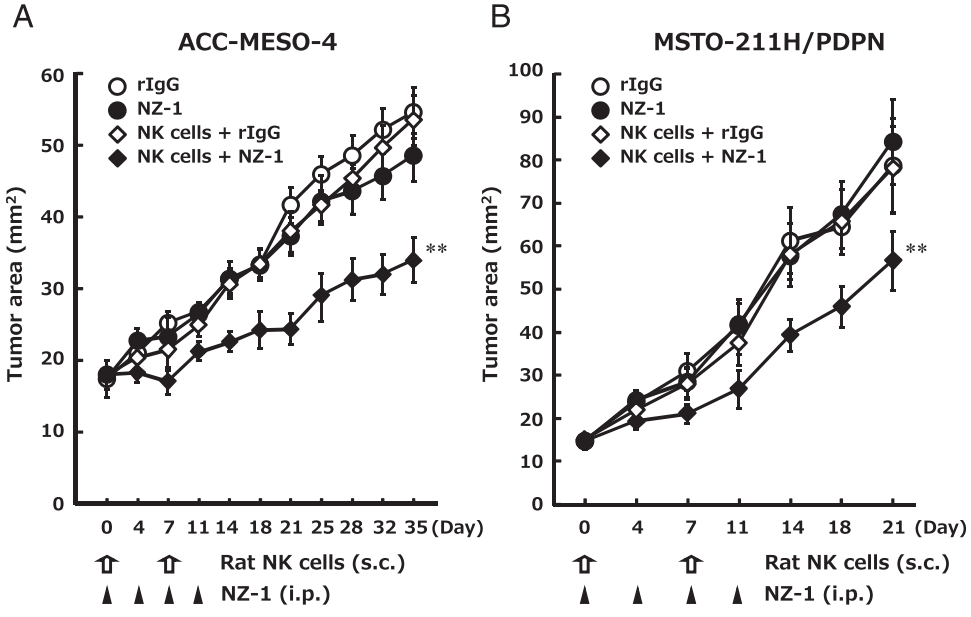

FIGURE 5. Antitumor activity of NZ-1 against MPM cells in vivo. SCID mice ($n = 5$) were injected s.c. with 4.0×10^6 ACC-MESO-4 cells (**A**) or 1.0×10^6 MSTO-211H/PDPN cells (**B**). NZ-1 (100 μg) or control rat IgG (rIgG; 100 μg) injection (i.p.) was continued twice a week for 2 wk. Rat NK ($CD161a^+$) cell (1.0×10^5 cells) injection (s.c.) around the tumors continued weekly for 2 wk. $^{**}p < 0.01$ versus control (values are means ± SE).

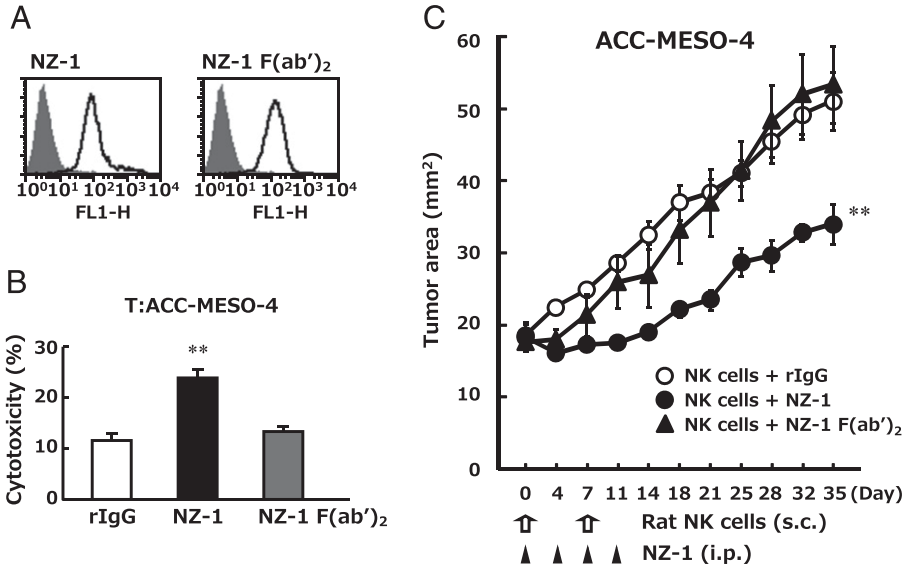

FIGURE 6. Critical contribution of Fc portion to antitumor activity of NZ-1. (**A**) Binding ability of NZ-1 F(ab′)$_2$ fragment to podoplanin on the cell surface was compared with that of NZ-1 by FACS analysis. (**B**) ADCC activity against ACC-MESO-4 was evaluated by [^{51}Cr]release assay in the presence of control rat IgG (rIgG), NZ-1, or NZ-1 F(ab′)$_2$ fragment with rat splenocytes. (**C**) Antitumor effect of NZ-1 (100 μg), NZ-1 F(ab′)$_2$ fragment (67.5 μg), or control rIgG (100 μg) injection (i.p.) was evaluated using ACC-MESO-4 s.c. xenograft SCID mouse model ($n = 5$). $^{**}p < 0.01$ versus control (values are means ± SE).

6B). Moreover, i.p. injection of NZ-1 F(ab′)$_2$ fragment unalterably showed no effect on tumor growth of ACC-MESO-4 compared with intact NZ-1, even when rat NK cells were simultaneously administered (Fig. 6C).

In vivo accumulation of injected NZ-1 to MPM xenograft in SCID mice

Next, we investigated the accumulation of injected NZ-1 on s.c. podoplanin-positive MPM tumor in SCID mouse model. As shown in Fig. 7A, Xenolight CF770-labeled NZ-1 accumulated on s.c. ACC-MESO-4 after single i.p. injection. Quantification of accumulation to the tumor of NZ-1 or control rat IgG showed a peak of the accumulation of NZ-1 on day 5, and the accumulation could be detected over 3 wk (Fig. 7B).

Immunostaining of podoplanin expressing in MPM and normal tissue with a novel rat-human chimeric anti-human podoplanin Ab NZ-8

Because it was demonstrated that NZ-1 showed antitumor activity through ADCC mediated by rat NK cells, to apply targeted therapy

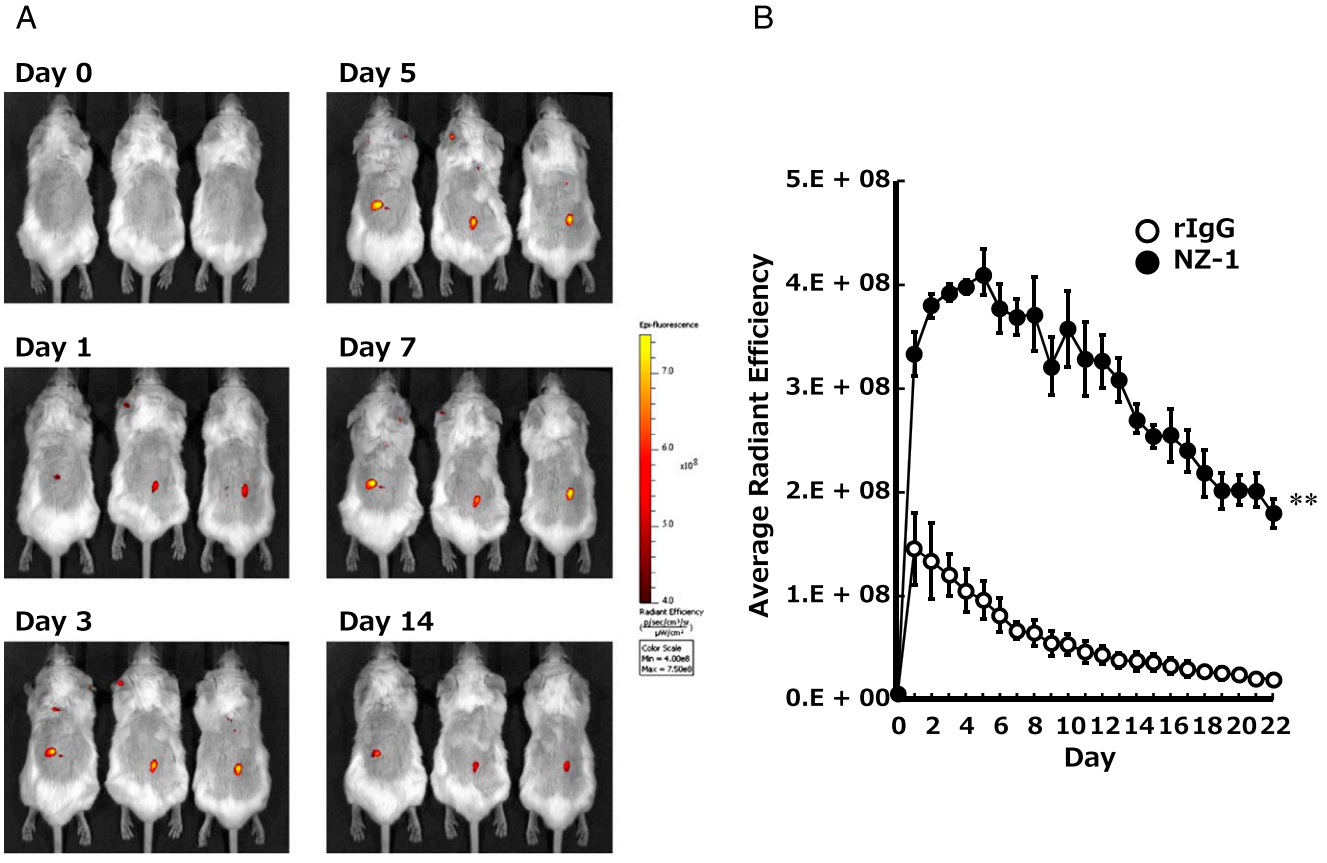

FIGURE 7. In vivo fluorescence imaging of NZ-1 in MPM xenograft model in SCID mice. (**A**) Fluorescence-labeled NZ-1 (100 μg) or control rat IgG (rIgG; 100 μg) was injected once i.p. to ACC-MESO-4 s.c. xenograft SCID mouse model ($n = 3$). (**B**) Accumulation of fluorescence in s.c. tumors was calculated and analyzed using IVIS Spectrum (Caliper Life Sciences) every day after the labeling Ab injection. $^{**}p < 0.01$ versus control (values are means ± SE).

to podoplanin with Ab in a clinic, we generated the chimeric Ab by fusing the V_H and V_L regions of rat Ab (NZ-1) with the C_H and C_L regions of human IgG_1, respectively (Fig. 8A). As shown in Fig. 8B and 8C, NZ-8, a novel rat-human chimeric anti-human podoplanin Ab, could recognize the podoplanin expressing in MPM like NZ-1 by flow cytometry as well as immunohistochemistry. Moreover, to confirm the recognition pattern of NZ-8 to podoplanin, the lysate of MPM cells were subjected to Western blotting. As shown in Fig. 8D, NZ-8 could detect the ladder bands of podoplanin. However, the recognizing pattern of NZ-8 was different from that of D2-40. Thinking of clinical application of NZ-8, the recognition of podoplanin expressing in normal tissue by NZ-8 is quite important. Therefore, we examined the staining pattern of podoplanin expressing in normal tissue such as lymphatic vessels, alveolar epithelial cells, and podocytes in the kidney by immunohistochemistry with NZ-8 because these tissues have been reported to express podoplanin. As shown in Fig. 8E, NZ-8 preferentially recognized the podoplanin expressing in MPM, but not in normal tissues including lymphatic vessels, alveolar epithelial cells, and podocytes. However, D2-40 strongly detected the podoplanin expressing in lymphatic vessels as compared with MPM tissues.

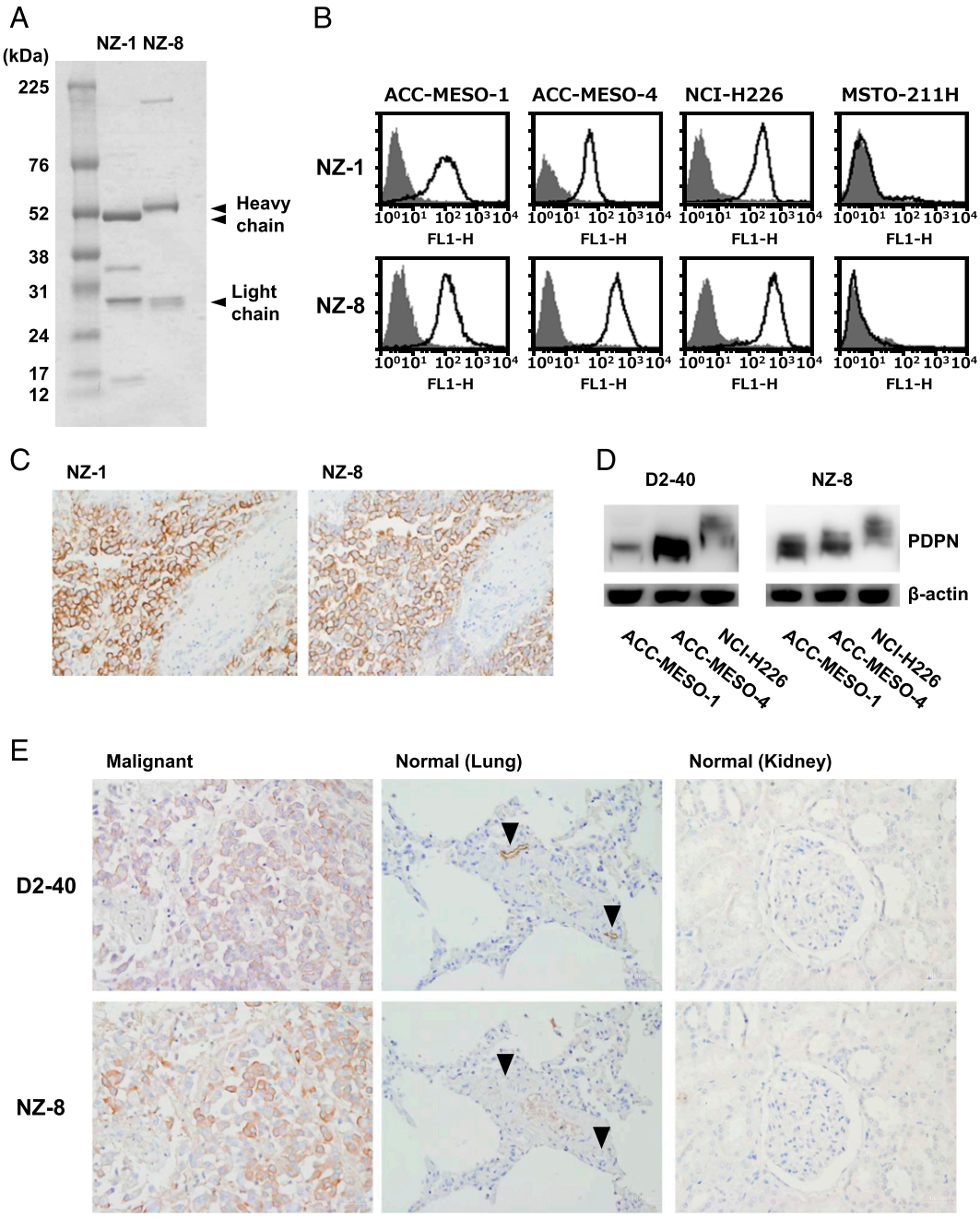

FIGURE 8. Immunostaining of podoplanin expressing in MPM and normal tissue with NZ-8. (**A**) SDS-PAGE of NZ-1 and NZ-8. SDS-PAGE using 5–20% gel was performed for purified NZ-1 and NZ-8 under the reducing condition. (**B**) Expression of podoplanin in MPM cell lines was detected by flow cytometry. MPM cell lines were stained with NZ-1 or NZ-8 (bold line) and control IgG (hatched area). (**C**) Immunohistochemistry demonstrated the detection of podoplanin expression using the tissue array. Tissues were stained with NZ-1 (1 μg/ml) or NZ-8 (1 μg/ml) (original magnification ×200). (**D**) Podoplanin (PDPN) protein in MPM cell lines was recognized by Western blotting proved with D2-40 (1:500) or NZ-8 (0.1 μg/ml). (**E**) The expression of podoplanin was examined in lymphatic vessels (arrowheads) and type I alveolar epithelium (lung) and podocyte (kidney) as well as MM using the tissue array. The slides of the tissue array were stained with D2-40 (1:500) or NZ-8 (0.1 μg/ml) (original magnification ×200).

In vitro and in vivo antitumor activity of NZ-8 against MPM cells

We further assessed whether NZ-8 can induce antitumor effect against MPM cells mediated by human MNC as effector cells. As shown in Fig. 9A, ADCC against MPM cell lines was not exhibited by NZ-1 with human MNC, whereas NZ-8 showed the induction of a significant level of ADCC mediated by human MNCs against podoplanin-positive MPM cells but not podoplanin-negative MPM cells. CDC was also induced by NZ-8 against ACC-MESO-4 and NCI-H226, which was significantly higher than that of NZ-1 (Fig. 9B). Further effector cell analysis of ADCC clearly demonstrated that human NK ($CD56^+$) cells, but not human monocytes ($CD14^+$), could induce ADCC by NZ-8 (Fig. 9C). Using the xenograft model of ACC-MESO-4 in SCID mice, the tumor growth was also significantly inhibited by treatment with NZ-8 and human NK ($CD56^+$) cells (Fig. 9D). By contrast, no antitumor effects were shown by the injection of NZ-8 or human NK ($CD56^+$) cells alone. Furthermore, administration of NZ-1 did not show any antitumor effects when human NK ($CD56^+$) cells were used as an effector cells (Fig. 9E).

Discussion

In the current study, we have demonstrated that a rat anti-human podoplanin mAb, NZ-1, possesses potent ADCC mediated by rat NK cells and CDC activity and mediates in vivo therapeutic antitumor activity against MPM in SCID mice. Moreover, we have also shown that a novel rat-human chimeric anti-human podoplanin Ab, NZ-8, effectively induces ADCC mediated by human NK cells and CDC and mediates in vivo antitumor activity against MPM cells. Furthermore, NZ-8 preferentially recognized the podoplanin expressing in MPM than those in normal tissues. These results strongly suggest the possible clinical application of anti-human podoplanin Ab against MPM.

In this study, we found that podoplanin was expressed on 73% of MPM cell lines including 33% of high-expression and 92% of MM tissues, which is consistent with previous studies (46–48). Furthermore, NZ-8 could recognize the expression of podoplanin in MPM like NZ-1. Compared with other mesothelioma-associated Ags such as calretinin, thrombomodulin, cytokeratin 5, WT1, and mesothelin in previous studies (47–49), the frequency of expression of podoplanin is the same or higher than that of others, suggesting that podoplanin could be a novel immunological target for MPM therapy. In contrast, although it was reported that podoplanin was expressed in lymphatic vessels and type I alveolar epithelium and podocyte (15–17), NZ-8 could not detect the expression of podoplanin in lymphatic vessels when it was used at the lower concentration of 0.1 μg/ml, which could still recognize the podoplanin in MPM tissues and induce the ADCC and CDC reactions. This staining pattern of NZ-8 is quite different from that

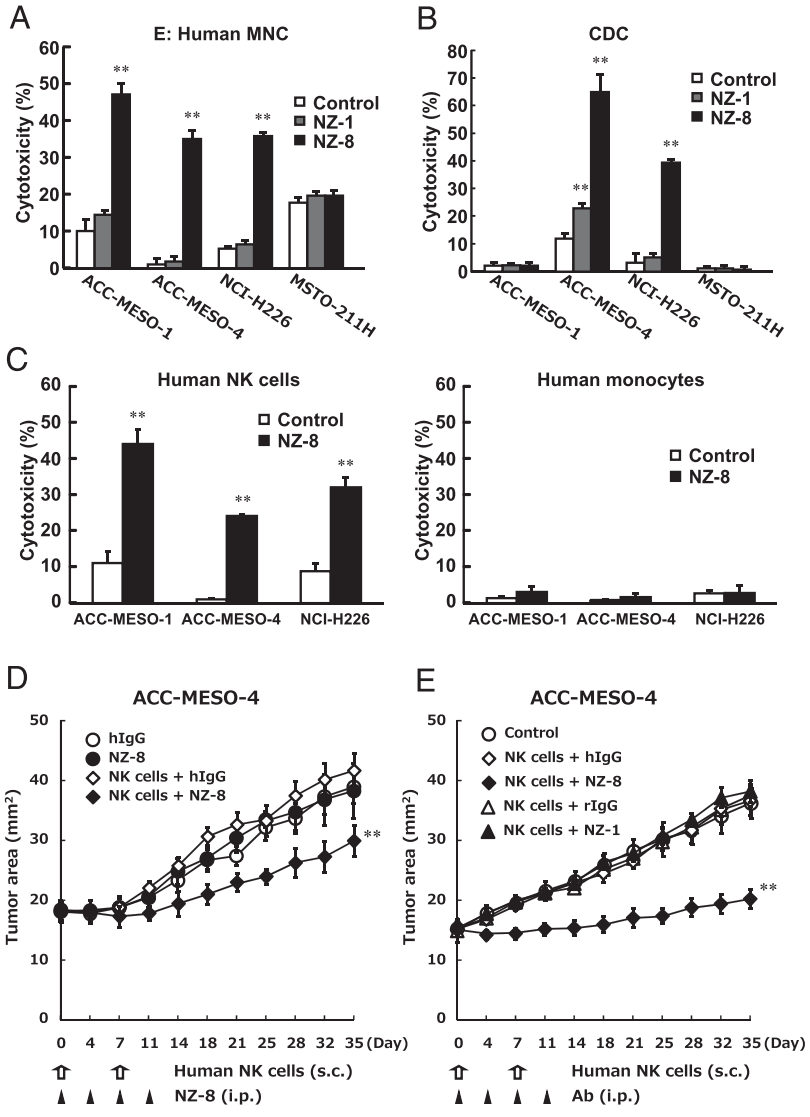

FIGURE 9. Antitumor activity of NZ-8 in vitro and in vivo. (**A**) ADCC induced by human MNC against MPM cell lines, ACC-MESO-1, ACC-MESO-4, NCI-H226, and MSTO-211H, was determined with 6-h [^{51}Cr]release assay at the E:T ratio of 100 in the presence of 1 μg/ml NZ-1 or NZ-8. (**B**) CDC activity was demonstrated by [^{51}Cr]release assay. The experimental condition was the same as for Fig. 2D. (**C**) Human NK cells are the main effector cells in ADCC activity of NZ-8. NK ($CD56^+$) cells or monocytes ($CD14^+$) were isolated from human MNC by AutoMACS. ADCC activity of 1 μg/ml NZ-8 mediated by NK ($CD56^+$) cells or monocytes ($CD14^+$) was evaluated by 6-h [^{51}Cr]release assay at E:T ratio of 10 or 50. SCID mice ($n = 5$) were injected s.c. with 4.0×10^6 ACC-MESO-4 cells. NZ-8 (100 μg) or human IgG (hIgG; 100 μg) (**D**), and NZ-1 (100 μg), NZ-8 (100 μg), or rat IgG (rIgG; 100 μg), and human IgG (hIgG; 100 μg) (**E**) injection (i.p.) was continued twice a week for 2 wk. Human NK ($CD56^+$) cell (1.0×10^5 cells) injection (s.c.) around the tumors continued weekly for 2 wk. $^{**}p < 0.01$ versus control (values are means ± SE).

of D2-40, which has been frequently used as an anti-podoplanin Ab in many studies (46, 47, 50). The reason why NZ-8 preferentially recognizes the podoplanin expressing in MPM, but not in normal tissues, is still unclear. However, it might be due to the difference in the epitopes recognized by each Ab in addition to the difference in the expression level of podoplanin between MPM and normal tissues, because we have shown that the epitope recognized by NZ-1 is platelet aggregation-stimulating domain-2/3, and the epitope of D2-40 is platelet aggregation-stimulating 1/2 (32). In the current study, it is considered that the recognition pattern of NZ-8, which possesses V_H and V_L of NZ-1, was also different from that of D2-40.

Originally, NZ-1 showed high binding affinity against podoplanin ($K_D = 1.2 \times 10^{-10}$ M) (33). In addition, it has been demonstrated that NZ-1 suppresses podoplanin-induced pulmonary metastasis through inhibiting platelet aggregation (27). In the current study, NZ-1 showed other effector functions, for ADCC and CDC. Recently, therapeutic Abs have been classified into three classes (34), in which class I Abs are defined to possess ADCC and CDC and ranked in the highly potential category, especially for cancer immunotherapy. On the basis of this concept, NZ-1 seems to be ranked as a highly potent therapeutic Ab because it has effector functions such as ADCC and CDC in addition to preventing metastasis by inhibiting platelet aggregation.

ADCC activity of NZ-1 has not been reported because NZ-1 did not show any ADCC activity mediated by murine splenocytes or human MNCs. However, when ADCC of NZ-1 was examined using rat splenocytes, significant ADCC activity was detected. To use rat splenocytes as effector cells is unusual to evaluate the ADCC activity of Ab; however, other studies have also reported that, in special cases, rat splenocytes are more useful than murine ones for testing the ADCC activity of rat mAb (51, 52). If the Ab has potency to induce the ADCC mediated by effector cells of several species except for humans effectively, it would be possible to prepare chimeric or humanized Ab that induces ADCC mediated by human effector cells. Therefore, from our study, it is also noted that rat splenocytes have the same importance to screen the ADCC activity of Ab as human MNC or mouse splenocytes.

In vivo experiments have shown that NZ-1 reduces the tumor growth of s.c. inoculated cell lines of both ACC-MESO-4 and MSTO-211H/PDPN, suggesting that NZ-1 possesses antitumor effects against MPM as well. In addition, it is very important that antitumor effects of NZ-1 were observed against established tumors, indicating that treatment with NZ-1 was apparently therapeutic, not preventive. Previously, we reported that NZ-1 directly inhibits podoplanin-dependent tumor metastasis in vivo (27). By contrast, in this study, administration of NZ-1 alone had no effect to reduce the podoplanin-positive MPM cell growth in SCID mice. The suppressive effects on tumor growth of NZ-1 are required for the administration with rat NK cells, probably as immune effector cells. In addition, NZ-1 $F(ab')_2$ fragment induced neither ADCC in vitro nor antitumor effect in vivo, which supports the notion that interaction between Fc portion of the Ab and FcR of the effector cell leads to the antitumor effect of NZ-1. Moreover, in vivo fluorescence imaging results have demonstrated that injected NZ-1 specifically accumulates to s.c. ACC-MESO-4. Recent study has shown that tumor accumulation of trastuzumab, which is an anti-Her2 Ab widely used against Her2-positive breast cancer in a clinical context, peaked at 24 h and decreased at the same rate as the baseline after 24 h in SCID mice model (53). By contrast, in this study, specific accumulation of NZ-1 peaked at day 5 and could continue over 3 wk after a single injection. Recently, we have also shown that NZ-1 was selectively accumulated to podoplanin-positive glioblastoma but not normal tissues (33). Therefore, it was estimated that NZ-1 has strong binding affinity and specific accumulation potential against target Ags. These results indicated that NZ-1 might have strong antitumor effects against MPM in vivo by ADCC.

Finally, we have shown that NZ-8, a novel rat-human chimeric anti-human podoplanin Ab, generated from NZ-1 has the potency to induce ADCC against MPM cells mediated by human NK cells as effector cells. Interestingly, the level of ADCC and CDC of NZ-8 was significantly higher than that of NZ-1. Moreover, NZ-8 has the promising antitumor effects against MPM cells mediated by human NK cells in vivo, in contrast to administration of NZ-1 with human NK cells, which did not induce any antitumor effects. In addition, NZ-8 preferentially detected the podoplanin expressing in MPM, but not in normal tissues.

In conclusion, we found that both NZ-1 and NZ-8 possess potent and therapeutic antitumor effects based on ADCC against MPM in an SCID mouse model. Importantly, NZ-8 could induce higher ADCC mediated by human NK cells in addition to CDC as compared with NZ-1. Based on the ability of NZ-8, which preferentially recognizes the podoplanin expressing in MPM, but not in normal tissues, the current study suggests that targeting therapy to podoplanin using NZ-8 might be useful for patients with MPM as a novel immunotherapy.

Acknowledgments

We thank Tomoko Oka, Imi Saito, Ryo Yanagiya, Shunpei Morita, Kana Nasu, Hiroko Sasaki, Sachiko Suzuki, and Junko Aita for excellent technical assistance.

Disclosures

The authors have no financial conflicts of interest.

References

1. Robinson, B. W., and R. A. Lake. 2005. Advances in malignant mesothelioma. *N. Engl. J. Med.* 353: 1591–1603.
2. Pelucchi, C., M. Malvezzi, C. La Vecchia, F. Levi, A. Decarli, and E. Negri. 2004. The Mesothelioma epidemic in Western Europe: an update. *Br. J. Cancer* 90: 1022–1024.
3. Murayama, T., K. Takahashi, Y. Natori, and N. Kurumatani. 2006. Estimation of future mortality from pleural malignant mesothelioma in Japan based on an age-cohort model. *Am. J. Ind. Med.* 49: 1–7.
4. Ray, M., and H. L. Kindler. 2009. Malignant pleural mesothelioma: an update on biomarkers and treatment. *Chest* 136: 888–896.
5. Vogelzang, N. J., J. J. Rusthoven, J. Symanowski, C. Denham, E. Kaukel, P. Ruffie, U. Gatzemeier, M. Boyer, S. Emri, C. Manegold, et al. 2003. Phase III study of pemetrexed in combination with cisplatin versus cisplatin alone in patients with malignant pleural mesothelioma. *J. Clin. Oncol.* 21: 2636–2644.
6. Scherpereel, A., P. Astoul, P. Baas, T. Berghmans, H. Clayson, P. de Vuyst, H. Dienemann, F. Galateau-Salle, C. Hennequin, G. Hillerdal, et al; European Respiratory Society/European Society of Thoracic Surgeons Task Force. 2010. Guidelines of the European Respiratory Society and the European Society of Thoracic Surgeons for the management of malignant pleural mesothelioma. *Eur. Respir. J.* 35: 479–495.
7. Inamoto, T., T. Yamada, K. Ohnuma, S. Kina, N. Takahashi, T. Yamochi, S. Inamoto, Y. Katsuoka, O. Hosono, H. Tanaka, et al. 2007. Humanized anti-CD26 monoclonal antibody as a treatment for malignant mesothelioma tumors. *Clin. Cancer Res.* 13: 4191–4200.
8. Inami, K., M. Abe, K. Takeda, Y. Hagiwara, M. Maeda, T. Segawa, M. Suyama, S. Watanabe, and O. Hino. 2010. Antitumor activity of anti-C-ERC/mesothelin monoclonal antibody in vivo. *Cancer Sci.* 101: 969–974.
9. Krug, L. M., T. Dao, A. B. Brown, P. Maslak, W. Travis, S. Bekele, T. Korontsvit, V. Zakhaleva, J. Wolchok, J. Yuan, et al. 2010. WT1 peptide vaccinations induce CD4 and CD8 T cell immune responses in patients with mesothelioma and non-small cell lung cancer. *Cancer Immunol. Immunother.* 59: 1467–1479.
10. Hassan, R., S. J. Cohen, M. Phillips, I. Pastan, E. Sharon, R. J. Kelly, C. Schweizer, S. Weil, and D. Laheru. 2010. Phase I clinical trial of the chimeric anti-mesothelin monoclonal antibody MORAb-009 in patients with mesothelin-expressing cancers. *Clin. Cancer Res.* 16: 6132–6138.
11. Kato, Y., N. Fujita, A. Kunita, S. Sato, M. Kaneko, M. Osawa, and T. Tsuruo. 2003. Molecular identification of Aggrus/T1alpha as a platelet aggregation-inducing factor expressed in colorectal tumors. *J. Biol. Chem.* 278: 51599–51605.
12. Kaneko, M. K., Y. Kato, T. Kitano, and M. Osawa. 2006. Conservation of a platelet activating domain of Aggrus/podoplanin as a platelet aggregation-inducing factor. *Gene* 378: 52–57.

13. Kaneko, M., Y. Kato, A. Kunita, N. Fujita, T. Tsuruo, and M. Osawa. 2004. Functional sialylated O-glycan to platelet aggregation on Aggrus (T1alpha/Podoplanin) molecules expressed in Chinese hamster ovary cells. *J. Biol. Chem.* 279: 38838–38843.
14. Hatakeyama, K., M. K. Kaneko, Y. Kato, T. Ishikawa, K. Nishihira, Y. Tsujimoto, Y. Shibata, Y. Ozaki, and Y. Asada. 2012. Podoplanin expression in advanced atherosclerotic lesions of human aortas. *Thromb. Res.* 129: e70–e76.
15. Breiteneder-Geleff, S., K. Matsui, A. Soleiman, P. Meraner, H. Poczewski, R. Kalt, G. Schaffner, and D. Kerjaschki. 1997. Podoplanin, novel 43-kd membrane protein of glomerular epithelial cells, is down-regulated in puromycin nephrosis. *Am. J. Pathol.* 151: 1141–1152.
16. Breiteneder-Geleff, S., A. Soleiman, H. Kowalski, R. Horvat, G. Amann, E. Kriehuber, K. Diem, W. Weninger, E. Tschachler, K. Alitalo, and D. Kerjaschki. 1999. Angiosarcomas express mixed endothelial phenotypes of blood and lymphatic capillaries: podoplanin as a specific marker for lymphatic endothelium. *Am. J. Pathol.* 154: 385–394.
17. Vanderbilt, J. N., L. Allen, R. F. Gonzalez, Z. Tigue, J. Edmondson, D. Ansaldi, A. M. Gillespie, and L. G. Dobbs. 2008. Directed expression of transgenes to alveolar type I cells in the mouse. *Am. J. Respir. Cell Mol. Biol.* 39: 253–262.
18. Kimura, N., and I. Kimura. 2005. Podoplanin as a marker for mesothelioma. *Pathol. Int.* 55: 83–86.
19. Kato, Y., M. Kaneko, M. Sata, N. Fujita, T. Tsuruo, and M. Osawa. 2005. Enhanced expression of Aggrus (T1alpha/podoplanin), a platelet-aggregation-inducing factor in lung squamous cell carcinoma. *Tumour Biol.* 26: 195–200.
20. Kato, Y., I. Sasagawa, M. Kaneko, M. Osawa, N. Fujita, and T. Tsuruo. 2004. Aggrus: a diagnostic marker that distinguishes seminoma from embryonal carcinoma in testicular germ cell tumors. *Oncogene* 23: 8552–8556.
21. Suzuki, H., Y. Kato, M. K. Kaneko, Y. Okita, H. Narimatsu, and M. Kato. 2008. Induction of podoplanin by transforming growth factor-beta in human fibrosarcoma. *FEBS Lett.* 582: 341–345.
22. Mishima, K., Y. Kato, M. K. Kaneko, R. Nishikawa, T. Hirose, and M. Matsutani. 2006. Increased expression of podoplanin in malignant astrocytic tumors as a novel molecular marker of malignant progression. *Acta Neuropathol.* 111: 483–488.
23. Wicki, A., F. Lehembre, N. Wick, B. Hantusch, D. Kerjaschki, and G. Christofori. 2006. Tumor invasion in the absence of epithelial-mesenchymal transition: podoplanin-mediated remodeling of the actin cytoskeleton. *Cancer Cell* 9: 261–272.
24. Martín-Villar, E., B. Fernández-Muñoz, M. Parsons, M. M. Yurrita, D. Megías, E. Pérez-Gómez, G. E. Jones, and M. Quintanilla. 2010. Podoplanin associates with CD44 to promote directional cell migration. *Mol. Biol. Cell* 21: 4387–4399.
25. Martín-Villar, E., D. Megías, S. Castel, M. M. Yurrita, S. Vilaró, and M. Quintanilla. 2006. Podoplanin binds ERM proteins to activate RhoA and promote epithelial-mesenchymal transition. *J. Cell Sci.* 119: 4541–4553.
26. Kunita, A., T. G. Kashima, Y. Morishita, M. Fukayama, Y. Kato, T. Tsuruo, and N. Fujita. 2007. The platelet aggregation-inducing factor aggrus/podoplanin promotes pulmonary metastasis. *Am. J. Pathol.* 170: 1337–1347.
27. Kato, Y., M. K. Kaneko, A. Kunita, H. Ito, A. Kameyama, S. Ogasawara, N. Matsuura, Y. Hasegawa, K. Suzuki-Inoue, O. Inoue, et al. 2008. Molecular analysis of the pathophysiological binding of the platelet aggregation-inducing factor podoplanin to the C-type lectin-like receptor CLEC-2. *Cancer Sci.* 99: 54–61.
28. Tsuneki, M., S. Maruyama, M. Yamazaki, J. Cheng, and T. Saku. 2012. Podoplanin expression profiles characteristic of odontogenic tumor-specific tissue architectures. *Pathol. Res. Pract.* 208: 140–146.
29. Yuan, P., S. Temam, A. El-Naggar, X. Zhou, D. D. Liu, J. J. Lee, and L. Mao. 2006. Overexpression of podoplanin in oral cancer and its association with poor clinical outcome. *Cancer* 107: 563–569.
30. Hoshino, A., G. Ishii, T. Ito, K. Aoyagi, Y. Ohtaki, K. Nagai, H. Sasaki, and A. Ochiai. 2011. Podoplanin-positive fibroblasts enhance lung adenocarcinoma tumor formation: podoplanin in fibroblast functions for tumor progression. *Cancer Res.* 71: 4769–4779.
31. Kato, Y., M. K. Kaneko, A. Kuno, N. Uchiyama, K. Amano, Y. Chiba, Y. Hasegawa, J. Hirabayashi, H. Narimatsu, K. Mishima, and M. Osawa. 2006. Inhibition of tumor cell-induced platelet aggregation using a novel anti-podoplanin antibody reacting with its platelet-aggregation-stimulating domain. *Biochem. Biophys. Res. Commun.* 349: 1301–1307.
32. Ogasawara, S., M. K. Kaneko, J. E. Price, and Y. Kato. 2008. Characterization of anti-podoplanin monoclonal antibodies: critical epitopes for neutralizing the interaction between podoplanin and CLEC-2. *Hybridoma (Larchmt)* 27: 259–267.
33. Kato, Y., G. Vaidyanathan, M. K. Kaneko, K. Mishima, N. Srivastava, V. Chandramohan, C. Pegram, S. T. Keir, C. T. Kuan, D. D. Bigner, and M. R. Zalutsky. 2010. Evaluation of anti-podoplanin rat monoclonal antibody NZ-1 for targeting malignant gliomas. *Nucl. Med. Biol.* 37: 785–794.
34. Jiang, X. R., A. Song, S. Bergelson, T. Arroll, B. Parekh, K. May, S. Chung, R. Strouse, A. Mire-Sluis, and M. Schenerman. 2011. Advances in the assessment and control of the effector functions of therapeutic antibodies. *Nat. Rev. Drug Discov.* 10: 101–111.
35. Kawaguchi, K., H. Murakami, T. Taniguchi, M. Fujii, S. Kawata, T. Fukui, Y. Kondo, H. Osada, N. Usami, K. Yokoi, et al. 2009. Combined inhibition of MET and EGFR suppresses proliferation of malignant mesothelioma cells. *Carcinogenesis* 30: 1097–1105.
36. Yokoyama, A., N. Kohno, S. Fujino, H. Hamada, Y. Inoue, S. Fujioka, and K. Hiwada. 1994. Origin of heterogeneity of interleukin-6 (IL-6) levels in malignant pleural effusions. *Oncol. Rep.* 1: 507–511.
37. Taniguchi, T., S. Karnan, T. Fukui, T. Yokoyama, H. Tagawa, K. Yokoi, Y. Ueda, T. Mitsudomi, Y. Horio, T. Hida, et al. 2007. Genomic profiling of malignant pleural mesothelioma with array-based comparative genomic hybridization shows frequent non-random chromosomal alteration regions including JUN amplification on 1p32. *Cancer Sci.* 98: 438–446.
38. Giovannetti, E., P. A. Zucali, Y. G. Assaraf, L. G. Leon, K. Smid, C. Alecci, F. Giancola, A. Destro, L. Gianoncelli, E. Lorenzi, et al. 2011. Preclinical emergence of vandetanib as a potent antitumour agent in mesothelioma: molecular mechanisms underlying its synergistic interaction with pemetrexed and carboplatin. *Br. J. Cancer* 105: 1542–1553.
39. Li, Q., W. Wang, T. Yamada, K. Matsumoto, K. Sakai, Y. Bando, H. Uehara, Y. Nishioka, S. Sone, S. Iwakiri, et al. 2011. Pleural mesothelioma instigates tumor-associated fibroblasts to promote progression via a malignant cytokine network. *Am. J. Pathol.* 179: 1483–1493.
40. Wang, W., Y. Nishioka, S. Ozaki, A. Jalili, S. Abe, S. Kakiuchi, M. Kishuku, K. Minakuchi, T. Matsumoto, and S. Sone. 2009. HM1.24 (CD317) is a novel target against lung cancer for immunotherapy using anti-HM1.24 antibody. *Cancer Immunol. Immunother.* 58: 967–976.
41. Kuramoto, T., H. Goto, A. Mitsuhashi, S. Tabata, H. Ogawa, H. Uehara, A. Saijo, S. Kakiuchi, Y. Maekawa, K. Yasutomo, et al. 2012. Dll4-Fc, an inhibitor of Dll4-notch signaling, suppresses liver metastasis of small cell lung cancer cells through the downregulation of the NF-κB activity. *Mol. Cancer Ther.* 11: 2578–2587.
42. Kishuku, M., Y. Nishioka, S. Abe, J. Kishi, H. Ogino, Y. Aono, M. Azuma, K. Kinoshita, R. Batmunkh, H. Makino, et al. 2009. Expression of soluble vascular endothelial growth factor receptor-1 in human monocyte-derived mature dendritic cells contributes to their antiangiogenic property. [Published erratum appears in 2010. *J. Immunol.* 185: 2630.] *J. Immunol.* 183: 8176–8185.
43. Wang, W., Y. Nishioka, S. Ozaki, A. Jalili, V. K. Verma, M. Hanibuchi, S. Abe, K. Minakuchi, T. Matsumoto, and S. Sone. 2009. Chimeric and humanized anti-HM1.24 antibodies mediate antibody-dependent cellular cytotoxicity against lung cancer cells. *Lung Cancer* 63: 23–31.
44. Nishioka, Y., N. Nishimura, Y. Suzuki, and S. Sone. 2001. Human monocyte-derived and CD83(+) blood dendritic cells enhance NK cell-mediated cytotoxicity. *Eur. J. Immunol.* 31: 2633–2641.
45. Zou, P., S. Xu, S. P. Povoski, A. Wang, M. A. Johnson, E. W. Martin, Jr., V. Subramaniam, R. Xu, and D. Sun. 2009. Near-infrared fluorescence labeled anti-TAG-72 monoclonal antibodies for tumor imaging in colorectal cancer xenograft mice. *Mol. Pharm.* 6: 428–440.
46. Chu, A. Y., L. A. Litzky, T. L. Pasha, G. Acs, and P. J. Zhang. 2005. Utility of D2-40, a novel mesothelial marker, in the diagnosis of malignant mesothelioma. *Mod. Pathol.* 18: 105–110.
47. Ordóñez, N. G. 2006. The diagnostic utility of immunohistochemistry and electron microscopy in distinguishing between peritoneal mesotheliomas and serous carcinomas: a comparative study. *Mod. Pathol.* 19: 34–48.
48. Chirieac, L. R., G. S. Pinkus, J. L. Pinkus, J. Godleski, D. J. Sugarbaker, and J. M. Corson. 2011. The immunohistochemical characterization of sarcomatoid malignant mesothelioma of the pleura. *Am. J. Cancer Res.* 1: 14–24.
49. Yaziji, H., H. Battifora, T. S. Barry, H. C. Hwang, C. E. Bacchi, M. W. McIntosh, S. J. Kussick, and A. M. Gown. 2006. Evaluation of 12 antibodies for distinguishing epithelioid mesothelioma from adenocarcinoma: identification of a three-antibody immunohistochemical panel with maximal sensitivity and specificity. *Mod. Pathol.* 19: 514–523.
50. Raica, M., A. M. Cimpean, and D. Ribatti. 2008. The role of podoplanin in tumor progression and metastasis. *Anticancer Res.* 28: 2997–3006.
51. Bergman, I., P. H. Basse, M. A. Barmada, J. A. Griffin, and N. K. Cheung. 2000. Comparison of in vitro antibody-targeted cytotoxicity using mouse, rat and human effectors. *Cancer Immunol. Immunother.* 49: 259–266.
52. Caragine, T. A., M. Imai, A. B. Frey, and S. Tomlinson. 2002. Expression of rat complement control protein Crry on tumor cells inhibits rat natural killer cell-mediated cytotoxicity. *Blood* 100: 3304–3310.
53. Rudnick, S. I., J. Lou, C. C. Shaller, Y. Tang, A. J. Klein-Szanto, L. M. Weiner, J. D. Marks, and G. P. Adams. 2011. Influence of affinity and antigen internalization on the uptake and penetration of Anti-HER2 antibodies in solid tumors. *Cancer Res.* 71: 2250–2259.